

Protein patterning

DOI: 10.1002/sml.200700519

Protein Immobilization Without Purification via Dip-Pen Nanolithography**

Kyung Hee Kim, Jung Dong Kim, Young Jun Kim, Seong Ho Kang, Seung Yong Jung, and Hyungil Jung*

Protein immobilization with pattern is important for both functional and structural studies of molecular interactions, such as protein–protein and protein–ligand interactions, and as a high-throughput screening tool in proteomics and drug screening.^[1–4] Nanopatterning techniques, such as electron-beam lithography,^[5] scanning probe lithography,^[6] and dip-pen nanolithography (DPN),^[7–12] were developed to immobilize proteins at the nanoscale. Generally, immobilization of proteins to pendant functional groups on the surface involves coupling reactions, such as biotin–streptavidin,^[13–16] antigen–antibody,^[17] and protein–ligand (or protein–protein).^[18] Because these coupling reactions require tailored purified proteins, purification of the target protein was required. Difficulties associated with obtaining a diversity of purified proteins, a time-consuming and labor-intensive process, have no doubt limited the number of studies using functional protein arrays.^[19]

To overcome these problems, the protein in situ array (PISA)^[20] and nucleic acid programmable protein array (NAPPA),^[19] which combine a cell-free system for protein synthesis and simultaneous in situ surface immobilization, have been introduced. In both strategies, proteins are transcribed and translated by a cell-free system and immobilized in situ by means of epitope tags fused to the proteins. Although these approaches eliminate the need to express and purify proteins separately, they are not suitable for nanoscale fabrication, and

even PISA requires a greater volume of the reaction mixture to make the array than a general microarray technique. To the best of our knowledge, successful protein immobilization at the nanoscale without target protein purification has not yet been reported. The main challenge is the creation of the nanoscale pattern where the target protein is selectively immobilized from cell extracts. Herein, we report the fabrication of a nitrilotriacetic acid (NTA)/Ni²⁺ pattern via DPN for the selective binding of His-tagged target protein, constructed by insertion of a small histidine-coding gene at the end of the target protein gene. The in situ immobilization of His-tagged protein was confirmed by the selective immobilization of the His-tagged enhanced green fluorescent protein (EGFP) from *Escherichia coli* cell extracts without prior purification.

The Ni–His bond is commonly used in immobilized metal-affinity chromatography for the purification of His-tagged proteins,^[21] as the His-tag acts as a high-affinity ($K_d \approx 10^{-13}$) recognition site for NTA/Ni²⁺.^[22,23] Stone et al. first used Ni–His systems for protein immobilization at the nanoscale level.^[22,24] They directly attached poly-His-tagged peptides and proteins by electrochemical DPN on Ni/NTA-coated glass. However, surface roughness and nonuniformity of slides were not appropriate for nanoscale patterning. Moreover, the applied field, required for the transport of His-tagged peptides and proteins from the atomic force microscopy (AFM) probe to the substrate, can induce protein denaturation. Mirkin's group solved this problem by using thermally evaporated Ni substrates and directly deposited His-tagged proteins by DPN without an applied field.^[25] Although this direct deposition of proteins had the advantage of immobilizing different proteins on the same surface, the relatively large size of the proteins impaired their transport from the AFM probe to the surface via DPN. Also, metallic nickel surfaces require ionization by exposure to ambient conditions for 24 h prior to use.

In these previous studies, the entire nickel surface was used as a substrate for the immobilization of His-tagged proteins and, consequently, required purified proteins. These results suggest that the fabrication of a nickel pattern, onto which the His-tagged protein can selectively immobilize, is the critical and necessary step for the immobilization of His-tagged protein without purification of the target protein. The nickel pattern can be constructed through NTA, which is a tetradentate chelating ligand that occupies four of the six binding sites in the coordination sphere of the nickel ion, thus leaving two sites free to interact with the 6 × His-tag.^[26] The success of protein immobilization without purification of the target protein may depend on the successful fabrication of a NTA/Ni²⁺ pattern, onto which the His-tagged proteins from *E. coli* cell extracts can be immobilized after chelating with nickel (Figure 1).

The NTA pattern was fabricated by DPN. Figure 2 shows tapping-mode AFM images of NTA dot patterns, which were created at different Tween-20 concentrations at fixed relative humidity (RH; 60%) on MPTMS-functionalized glass. Because the surfactant concentration in the DPN ink is the critical systematic parameter in patterning partially hydrophobic surfaces, such as MPTMS,^[27] the effect of the Tween-20

[*] K. H. Kim, J. D. Kim, Prof. H. Jung

Department of Biotechnology
Yonsei University
Seoul 120-749 (Korea)
E-mail: hijung@yonsei.ac.kr

Prof. Y. J. Kim
Department of Food and Biotechnology
Korea University
Jochiwon 339-700 (Korea)

Prof. S. H. Kang
Department of Chemistry and
Research Institute of Physics and Chemistry (RINPAC)
Chonbuk National University
Jeonju 561-756 (Korea)

Dr. S. Y. Jung
Division of Chemistry and Chemical Engineering California Institute
of Technology
Pasadena, CA 91125 (USA)

[**] The authors thank Hye Jin Kang for the theoretical height calculation of the maleimido-C₃-NTA and Sungil Choi for kindly supplying the LysN-His-EGFP. This work was supported by a Korea Research Foundation Grant funded by the Korean Government (MOEHRD) (KRF-2006-331-D00177).

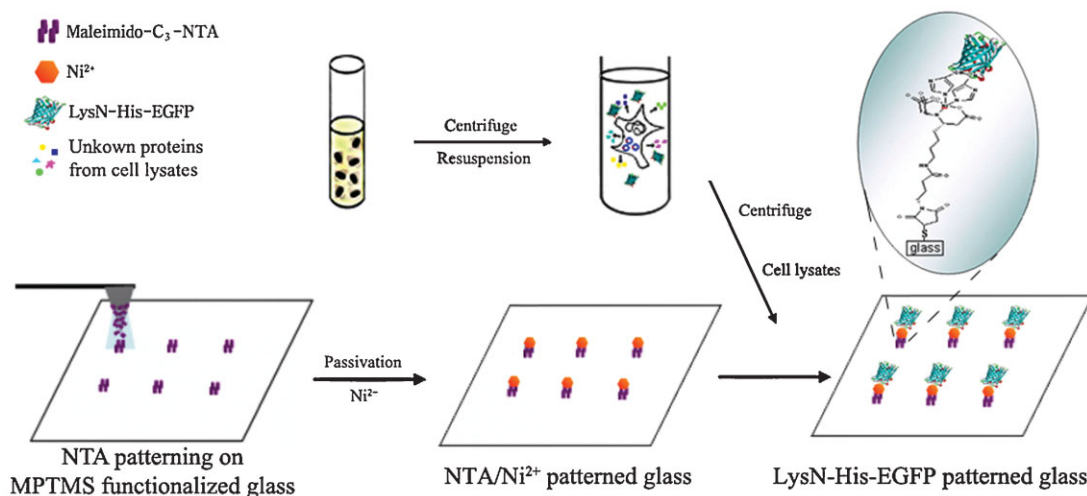


Figure 1. NTA/ Ni^{2+} patterning by DPN and selective immobilization of the His-tagged protein from cell lysates without prior purification on the NTA/ Ni^{2+} pattern. LysN = N-terminal domain of *E. coli* lysyl-tRNA synthetase; MPTMS = 3'-mercaptopropyltrimethoxysilane.

concentration on NTA transport was investigated. There were no consistent DPN patterns observed without the addition of Tween-20, even after 120 s; therefore, inks containing various percentages of Tween-20 (i.e., 0.001, 0.01, and 0.1%) were compared. As shown in Figure 2, the increase in dot diameter with tip–substrate contact time was greatest with the highest surfactant concentrations, as expected. At a given contact time, the dot diameter increased as the Tween-20 concentration increased. This dependence of surfactant concentration on dot diameter was related to the spreading parameter S .^[27] As water-based inks, such as NTA, will not completely wet the partially hydrophobic MPTMS surface, the added Tween-20 promotes the spreading of the ink on the surface by adsorption at both the solid/liquid (λ_{SL}) and liquid/vapor (λ_{LV}) interfaces, lowering surface tensions. These results suggest that the relative concentration of Tween-20 can be systematically varied in addition to other parameters, such as RH,

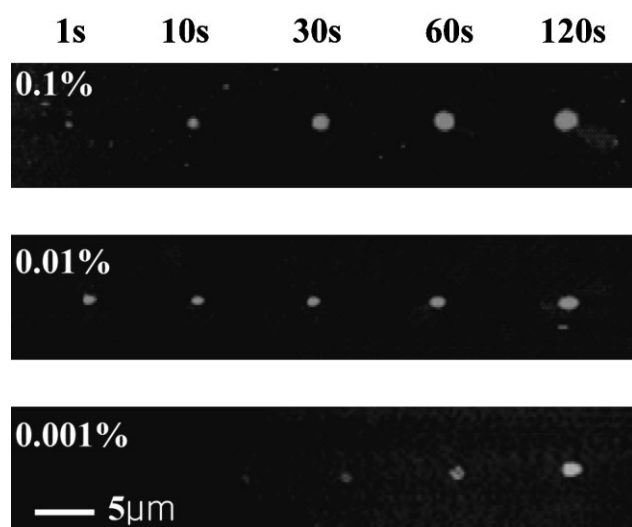


Figure 2. Tapping-mode AFM topographical images of maleimido- C_3 -NTA dot patterns on MPTMS-functionalized glass for the indicated tip–substrate contact times [s] at 60% RH. The ink included 0.001, 0.01, and 0.1% Tween-20.

temperature, scan speed, and force, to control the deposition of ink by DPN. Also, the dot diameter increased as the contact time increased at three different Tween-20 concentrations, consistent with previous DPN experiments in which the deposited ink molecules laterally diffused on the substrate as contact time increased.^[27]

Figure 3a shows the tapping-mode topographic image of a 5×2.5 - μm rectangular pattern of maleimido- C_3 -NTA, while

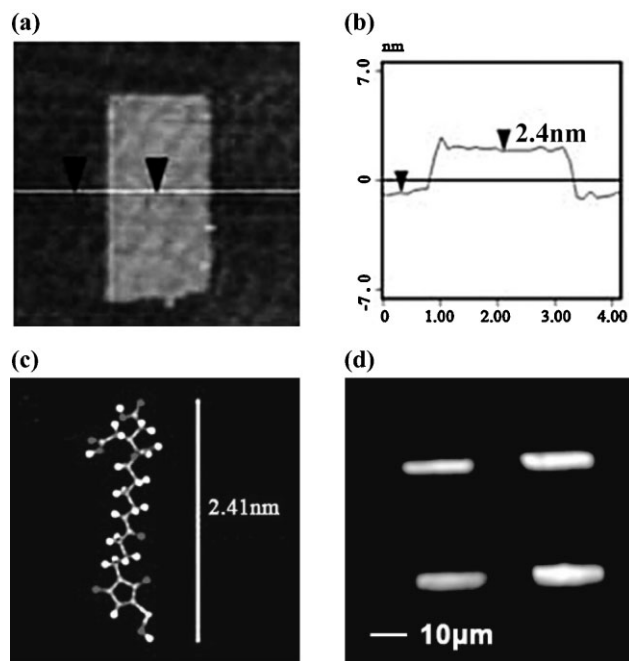


Figure 3. a) AFM topographical image of a 5×2.5 - μm rectangular pattern of maleimido- C_3 -NTA. The pattern was written at 62% RH and then immediately imaged in tapping mode. b) Corresponding average, cross-sectional height of a 5×2.5 - μm rectangular pattern of NTA. The height difference between the two arrows was 2.4 nm. c) Maleimido- C_3 -NTA structure and theoretical height by the Molecular Modeling Pro program. d) Fluorescence image of 20×5 - μm regions of maleimido- C_3 -NTA conjugated to Ni^{2+} and purified LysN-His-EGFP.

Figure 3b shows an average of cross-sectional traces of the height measured perpendicular to the top of the pattern. The theoretical length of maleimido- C_3 -NTA obtained by Molecular Modeling Pro (ChemSW) was 2.41 nm (Figure 3c), which indicates that maleimido- C_3 -NTA was most likely deposited as a monolayer. The NTA pattern was confirmed by fluorescence labeling studies using purified His-tagged EGFP after chelation with Ni^{2+} ions by incubation in nickel chloride (12 mg mL^{-1} , Sigma) for 15 min. We used the fusion molecule, LysN-His-EGFP, in which LysN was connected with EGFP through six consecutive histidine residues. Here, LysN prevented the formation of an inclusion body containing a reporter protein, such as EGFP, by binding to its cognate tRNA, which has a strong negative charge. This RNA-mediated, intramolecular chaperone (Cisperone) can increase the solubility and activity of the target protein on the immobilized surface. In this study, however, the LysN-His-EGFP fusion protein was used to test the selective immobilization of the His-tagged protein onto NTA/ Ni^{2+} patterns. The availability of pendant Ni^{2+} on DPN-patterned NTA for further coupling reactions was tested by introducing purified LysN-His-EGFP fusion protein. Figure 3d shows fluorescence images of four $20 \times 5\text{-}\mu\text{m}$ patterns of maleimido- C_3 -NTA/ Ni^{2+} conjugated to LysN-His-EGFP. The His-tagged fluorescent protein, LysN-His-EGFP, was specifically immobilized only onto NTA/ Ni^{2+} -patterned areas, and showed minimal nonspecific binding of LysN-His-EGFP onto unpatterned areas, as indicated by the relative fluorescence intensity between patterned regions and the background.

His-tagged protein purification using NTA/ Ni^{2+} columns has been broadly adopted by both the molecular biology and biochemistry communities. This selective binding of His-tagged proteins offers opportunities for the construction of protein immobilization on solid surfaces directly from crude cell lysates without prior purification of target proteins.^[28] Combined with the NTA/ Ni^{2+} pattern, these genetically modified His-tagged proteins represent a powerful approach

to the construction of protein patterns at the nanoscale with a single purification and immobilization step. This proof of concept was tested by the selective binding of LysN-His-EGFP from cell lysates to a NTA/ Ni^{2+} pattern.

The expression and purity of the LysN-His-EGFP protein were evaluated by sodium dodecyl sulfate–polyacrylamide gel electrophoresis (SDS-PAGE) of the cell lysates. The bands of the gel were stained with Coomassie brilliant blue. As a control, purified LysN-His-EGFP was also loaded onto the gel, and a band of the correct size corresponding to LysN-His-EGFP was observed (Figure 4a, lane C). Cell lysates, as expected, showed multiple bands. This finding indicated that the cell lysates contained mixtures of the unknown proteins as well as the target protein, LysN-His-EGFP (Figure 4a, lane L). Western blot analysis was carried out to confirm the expression of LysN-His-EGFP from the *E. coli* expression host, HMS174 (DE3) plysE (Figure 4b). For comparison, purified LysN-His-EGFP (51–53 kDa) was analyzed on Western blots as shown in Figure 4b (lane C). A nonspecific band (lane L), which has a molecular weight of 120 kDa, was observed in addition to LysN-His-EGFP. As the membrane was probed with mouse anti-His monoclonal antibodies, this nonspecific band suggests the presence of a naturally existing histidine-rich protein in the cell lysate.^[29] Cell lysates containing LysN-His-EGFP were incubated on 2×2 NTA/ Ni^{2+} patterns (500 nm) for 15 min. Figure 4c clearly shows the selective binding of the target protein, LysN-His-EGFP, from cell lysates on NTA/ Ni^{2+} patterns. This selective binding suggests that the NTA/ Ni^{2+} pattern can be used for in situ immobilization of His-tagged proteins from protein mixtures, especially from cell lysates.

This novel technique may also be applied to the creation of multiple protein patterns with various proteins by combining with the multiple spotting technique (MIST).^[30] MIST involves the immobilization of a binder onto a surface and the subsequent spotting of a second compound on the same spot as the immobilized binder. If NTA/ Ni^{2+} patterns are used

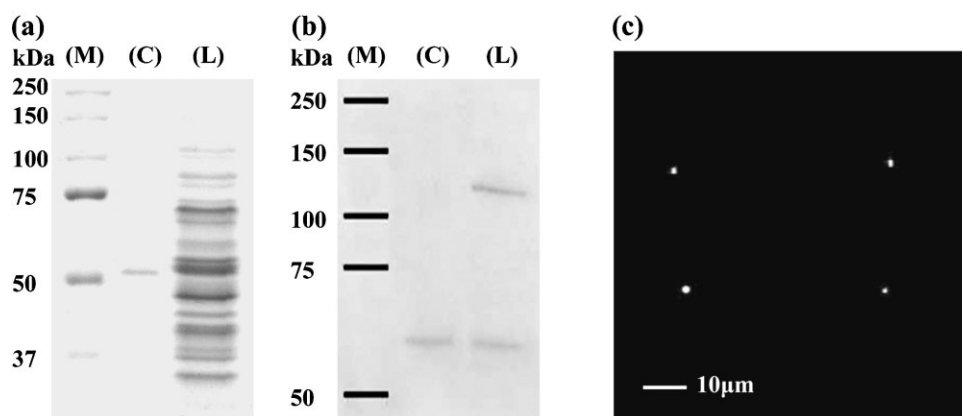


Figure 4. a) Purity of the His-tagged protein, LysN-His-EGFP, from cell lysates. Samples were loaded and stained on an SDS–polyacrylamide gel for analysis. Lane M is the size marker, lane C is the purified LysN-His-EGFP as a positive control, and lane L is cell lysate. b) Western blot analysis of total cell lysates from the *E. coli* expression host, HMS174 (DE3) plysE, for LysN-His-EGFP. Lane C is the purified LysN-His-EGFP as a positive control and lane L is cell lysate from HMS174 (DE3) plysE. c) Fluorescence image of four LysN-His-EGFP fusion proteins from cell lysates coupled to 500-nm spot regions of the NTA/ Ni^{2+} pattern.

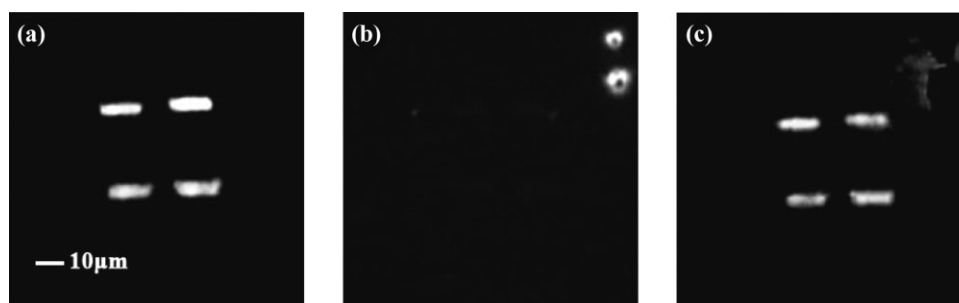


Figure 5. Test of reversibility of LysN-His-EGFP on NTA/Ni²⁺ patterns. Fluorescence images of a) LysN-His-EGFP coupled with NTA/Ni²⁺ patterns; b) after treatment with elution buffer containing 300 mM imidazole, 300 mM NaCl, and 50 mM NaH₂PO₄; c) after rebinding of LysN-His-EGFP.

as the first binder, as in MIST, a multiple pattern with an additional protein is possible by spotting a second His-tagged protein from different cell lysates on different NTA/Ni²⁺ patterns. Thus, the NTA/Ni²⁺ pattern may present opportunities for the construction of in situ protein immobilization without target protein purification.

One of the major advantages of the NTA/His-tag system is the reversible binding of His-tagged proteins to NTA/Ni²⁺; His-tagged proteins can be readily eluted under mild conditions.^[26,31] To demonstrate this reversible binding, we used a buffer containing imidazole, a known competitive inhibitor of NTA-His binding to Ni²⁺.^[21,32] Figure 5a shows fluorescence images of LysN-His-EGFP coupled with the NTA/Ni²⁺ pattern as described previously. We observed a decrease in fluorescence from the patterned regions by the addition of elution buffer (300 mM imidazole, 300 mM NaCl, and 50 mM NaH₂PO₄) after 3 min (Figure 5b). This loss of fluorescence may be caused by the detachment of LysN-His-EGFP from the NTA/Ni²⁺ pattern or of Ni²⁺ ions from the NTA pattern. The NTA-Ni²⁺ complex is reportedly strong enough for its nickel concentration to be unaffected by a 200 mM imidazole solution. This conclusion is consistent with the fact that the affinity of a given protein on nickel-loaded resins is dependent on the structure of the protein itself.^[33] Also, a NTA-His “unbinding” force (15–194 pN) was measured at the single-molecule level by a force–distance curve;^[34] this “unbinding” force was diminished by blocking experiments with imidazole, which suggests that the complex between the His-tagged protein and nickel is more fragile than the complex between nickel and the NTA group.

After washing the imidazole-treated NTA/Ni²⁺ pattern with phosphate-buffered saline (PBS), LysN-His-EGFP was incubated for 15 min with the NTA/Ni²⁺ pattern. Figure 5c shows the regeneration of LysN-His-EGFP binding on the NTA/Ni²⁺ pattern, although the fluorescence intensity decreased to 75% of the initial value. This decrease may be caused by desorption of the Ni. Roure et al. reported that the Ni concentration on the NTA surface was approximately 20–25% lower than its initial value after treatment with high concentrations of Ca²⁺ (100 mM), ethylenediaminetetraacetic acid (100 mM), or imidazole (200 mM).^[32] The NTA pattern could be simply regenerated by subsequent incubation in nickel chloride. Thus, the reversible binding of His-tagged biomolecules to metal-chelating molecules makes the screening

of different His-tagged proteins on the same surface possible in a rather straightforward modification of the experimental conditions.^[35]

In summary, we have fabricated maleimido-C₃-NTA patterns by DPN for the effective immobilization of His-tagged proteins, a widely used technique for the purification of target proteins. Also, we demonstrated that His-tagged proteins can be selectively immobilized onto NTA/Ni²⁺ patterns from cell lysates. The application of this chelating chemistry for protein immobilization offers several distinct advantages over biochemical recognition elements, such as antibodies or biotin/streptavidin (neutral avidin) systems: 1) orientation-controlled immobilization of His-tagged proteins could be very useful for the detection of biomolecular interactions at the nanoscale, which requires enhanced/maximized interactions between the immobilized biomolecules and ligands; 2) His-tags that bind to either the C or N terminus are commercially available for a large number of proteins; 3) the formation of a His-Ni²⁺ complex is a rapid reaction; 4) the reversibility of binding of His-tagged protein to NTA/Ni²⁺ patterns provides versatility for automated assay formats with different proteins on the same biochip; and 5) the selective binding of His-tagged proteins could provide a powerful tool for the in situ construction of protein patterns from cell lysates without purification of the target protein. These new methods, which use the NTA/Ni²⁺ pattern and small histidine-coding gene insertions at the end of the target protein gene, make it possible to construct target protein patterns without purification. As this addresses the primary challenge in the construction of protein chips, this technique is well suited for such preparation because of the selective, rapid, and orientation-controlled immobilization without prior protein purification.

Experimental Section

Substrates: Glass substrates (#1 coverslip, Marienfeld) were prepared by piranha cleaning (H₂O₂/H₂SO₄, 3:7, v/v) in a sonic cleaner (Branson) for 1 h. After extensive washing with deionized water (Millipore Gradient), MPTMS (Sigma) monolayers were introduced onto the clean substrate by silanization.^[36] This mercaptosilanized glass with a thiol group as the functional pendant group was used as the substrate for DPN writing.

DPN: A commercially available AFM tip (silicon nitride cantilever, 0.58 N m^{-1} , Digital Instruments) was cleaned with UV-tip cleaner (UV TipCleaner, BioForce), rinsed copiously with deionized water, and dried at 100°C . To facilitate maleimide-linked ink adsorption onto the AFM tip, the tip was coated with MPTMS ($3 \mu\text{L}$), which was evaporated at 120°C for 30 min in a 300-mL closed jar.^[10] Tips were then coated with DPN ink for 10 min in maleimido- $\text{C}_3\text{-NTA}$ (2 mg mL^{-1} , Dojindo) containing Tween-20 (Sigma–Aldrich) in $1\times$ PBS (Sigma). The AFM tip was blow-dried with compressed nitrogen gas. DPN experiments were performed using a bio-atomic force microscope (Nanoscope IIIa controller) from Digital Instruments. The RH was controlled between 45 and 70% by purged nitrogen gas that was bubbled through water in a large glove box. All DPN experiments were performed in contact mode, and patterns were imaged by either lateral force microscopy or tapping-mode AFM immediately after writing. The NTA pattern was produced by DPN at a scanning speed of $10 \mu\text{m s}^{-1}$ at 62% RH.

Surface modification: The unpatterned areas of the mercaptosilvanized glass surface were passivated with a 0.05 mM solution of polyethylene glycol–maleimide (ID Biochem) in $1\times$ PBS (1 mg mL^{-1}) to prevent nonspecific protein binding. To construct an active pattern for His-tagged protein immobilization, the NTA pattern was chelated with Ni^{2+} ions by incubation in nickel chloride (12 mg mL^{-1} , Sigma) for 15 min. Then, the NTA/ Ni^{2+} nanopatterns were treated with cell extracts that contained LysN-His-EGFP ($22 \mu\text{g mL}^{-1}$) for 15 min. After vigorous washing, the samples patterned in $1\times$ PBS were dried under nitrogen gas.

Pattern observation: Fluorescence was observed using an inverted epifluorescence microscope with a mercury arc lamp (IX71, Olympus). Images of fluorescence patterns were captured with a high-resolution, Peltier-cooled CCD camera (DP70, Olympus).

LysN-His-EGFP expression: The LysN-His-EGFP expression vector was transformed into the *E. coli* expression host, HMS174 (DE3) plysE. A single colony of transformants was selected and inoculated in Luria–Bertani (LB) medium (3 mL) containing ampicillin ($50 \mu\text{g mL}^{-1}$). After overnight incubation at 37°C , cells were cultured in fresh LB (20 mL) until the cell optical density reached $\text{O.D.}_{600} = 0.7$; cells were then induced with isopropyl- β -D-thiogalactopyranoside (1 mM). After incubation at 37°C for 4–5 h, cells were pelleted at 12 000 rpm for 10 min at 4°C , and the supernatant was removed. Cells were washed in $1\times$ PBS (2 mL) with mixing and pelleted under the same conditions as indicated above. After removal of the supernatant, the cells were resuspended in $1\times$ PBS (2 mL) and sonicated at 45% amplitude and 4°C . To obtain cell lysates containing LysN-His-EGFP, cells were pelleted at 12 000 rpm for 20 min at 4°C .

Western blot: After separation on a 10% SDS–polyacrylamide gel, proteins were transferred onto a nitrocellulose membrane using a semidry blotting system (Bio-Rad) in transfer buffer (248 mM Tris-base, 1.91 M glycine, and 20% methanol) for 80 min at 15 V. After blocking with 5% albumin (Amresco) in Tris-buffered saline (TBS) containing 0.1% Tween-20 (TBST) for 4 h, the membrane was probed with a mouse anti-His monoclonal antibody (Qiagen; 1:1000 dilution) for the detection of LysN-His-EGFP fusion protein. After washing in TBST for 60 min, the membrane was incubated with secondary antibody (horseradish peroxidase-conjugated mouse anti-IgG antibody; Sigma), washed, developed, and visualized by enhanced chemiluminescence (Roche).

Keywords:

dip-pen nanolithography · immobilization · pattern formation · proteins

- [1] J. W. Choi, Y. S. Nam, M. Fujihira, *Biotechnol. Bioprocess Eng.* **2004**, *9*, 76.
- [2] M. Lynch, C. Mosher, J. Huff, S. Nettikadan, J. Johnson, E. Henderson, *Proteomics* **2004**, *4*, 1695.
- [3] M. Lee, D. K. Kang, H. K. Yang, K. H. Park, S. Y. Choe, C. Kang, S. I. Chang, M. H. Han, I. C. Kang, *Proteomics* **2006**, *6*, 1094.
- [4] J. Kim, K. C. Han, Y. G. Yu, E. G. Yang, *Biochip J.* **2007**, *1*, 134.
- [5] P. M. Mendes, S. Jacke, K. Critchley, J. Plaza, Y. Chen, K. Nikitin, R. E. Palmer, J. A. Preece, S. D. Evans, D. Fitzmaurice, *Langmuir* **2004**, *20*, 3766.
- [6] R. Y. P. Lue, G. Y. J. Chen, Y. Hu, Q. Zhu, S. Q. Yao, *J. Am. Chem. Soc.* **2004**, *126*, 1055.
- [7] R. D. Piner, J. Zhu, F. Xu, S. Hong, C. A. Mirkin, *Science* **1999**, *283*, 661.
- [8] L. M. Demers, D. S. Ginger, S. J. Park, Z. Li, S. W. Chung, C. A. Mirkin, *Science* **2002**, *296*, 1836.
- [9] a) K. B. Lee, S. J. Park, C. A. Mirkin, J. C. Smith, M. Mrksich, *Science* **2002**, *295*, 1702; b) K. B. Lee, J. H. Lim, C. A. Mirkin, *J. Am. Chem. Soc.* **2003**, *125*, 5588.
- [10] H. Jung, R. Kulkarni, C. P. Collier, *J. Am. Chem. Soc.* **2003**, *125*, 12096.
- [11] D. S. Ginger, H. Zhang, C. A. Mirkin, *Angew. Chem.* **2004**, *116*, 30; *Angew. Chem. Int. Ed.* **2004**, *43*, 30.
- [12] D. S. Choi, S. H. Yun, Y. C. An, M. J. Lee, D. G. Kang, S. I. Chang, H. K. Kim, K. M. Kim, J. H. Lim, *Biochip J.* **2007**, *1*, 200.
- [13] J. N. Herron, W. Müller, M. Paudler, H. Riegler, H. Ringsdorf, P. A. Suci, *Langmuir* **1992**, *8*, 1413.
- [14] J. Spinke, M. Liley, H. J. Guder, L. Angermaier, W. Knoll, *Langmuir* **1993**, *9*, 1821.
- [15] M. E. Browning-Kelley, K. Waud-Mesthrige, V. Hari, G.-Y. Liu, *Langmuir* **1997**, *13*, 343.
- [16] G. B. Sigal, C. Bamdad, A. Barberis, J. Strominger, G. M. Whitesides, *Anal. Chem.* **1996**, *68*, 490.
- [17] D. J. Zhou, X. Z. Wang, L. Birch, T. Rayment, C. Abell, *Langmuir* **2003**, *19*, 10557.
- [18] J. K. Lee, Y. G. Kim, Y. S. Chi, W. S. Yun, I. S. Choi, *J. Phys. Chem. B* **2004**, *108*, 7665.
- [19] N. Ramachandran, E. Hainsworth, B. Bhullar, S. Eisenstein, B. Rosen, A. Y. Lau, J. C. Walter, J. LaBaer, *Science* **2004**, *305*, 86.
- [20] M. He, M. J. Taussig, *Nucleic Acids Res.* **2001**, *29*, 73.
- [21] M. Conti, G. Falini, B. Samorì, *Angew. Chem.* **2000**, *112*, 221; *Angew. Chem. Int. Ed.* **2000**, *39*, 215.
- [22] G. Agarwal, R. R. Naik, M. O. Stone, *J. Am. Chem. Soc.* **2003**, *125*, 7408.
- [23] L. R. Paborsky, K. E. Dunn, C. S. Gibbs, J. P. Dougherty, *Anal. Biochem.* **1996**, *234*, 60.
- [24] Y. Li, B. W. Maynor, J. Liu, *J. Am. Chem. Soc.* **2001**, *123*, 2105.
- [25] J. M. Nam, S. W. Han, K. B. Lee, X. Liu, M. A. Ratner, C. A. Mirkin, *Angew. Chem.* **2004**, *116*, 1266; *Angew. Chem. Int. Ed.* **2004**, *43*, 1246.
- [26] G. Zhen, D. Falconnet, E. Kuennemann, J. Vörös, N. D. Spencer, M. Textor, S. Zürcher, *Adv. Funct. Mater.* **2006**, *16*, 243.
- [27] H. Jung, C. K. Dalal, S. Kurz, P. Shah, C. P. Collier, *Nano Lett.* **2004**, *4*, 2171.
- [28] J. Maly, C. Di Meo, M. De Francesco, A. Masci, J. Masojidek, M. Sugiura, A. Volpe, R. Pilloton, *Bioelectrochemistry* **2004**, *63*, 271.
- [29] Z. Xu, S. Y. Lee, *Appl. Environ. Microbiol.* **1999**, *65*, 5142.
- [30] P. Angenendt, J. Glökler, Z. Konthur, H. Lehrach, D. Cahill, *Anal. Chem.* **2003**, *75*, 4368.
- [31] D. S. Waugh, *Trends Biotechnol.* **2005**, *23*, 316.
- [32] L. Nieba, A. Krebber, A. Pluckthun, *Anal. Biochem.* **1996**, *234*, 155.

- [33] O. D. Roure, C. D. Chouvy, J. Malthête, P. Silberzan, *Langmuir* **2003**, *19*, 4138.
- [34] F. Kienberger, G. Kada, H. J. Gruber, V. P. Pastushenko, C. Reiner, M. Trieb, H. G. Knaus, H. Schindler, P. Hinterdorfer, *Single Mol.* **2000**, *1*, 59.
- [35] L. Schmitt, M. Ludwig, H. E. Gaub, R. Tampé, *Biophys. J.* **2000**, *78*, 3275.
- [36] A. A. Krasnoslobodtsev, S. N. Smirnov, *Langmuir* **2002**, *18*, 3181.

Received: July 11, 2007
Revised: March 26, 2008
